CASE OF THE WEEK

PROFESSOR YASSER METWALLY

CLINICAL PICTURE

CLINICAL PICTURE:

A 40 years old female patient presented clinically with manifestations of increased intracranial pressure, long tract manifestations, ponto-medullary cranial nerve palsies. and cerebellar manifestations. Hearing was intact.

RADIOLOGICAL FINDINGS

RADIOLOGICAL FINDINGS:

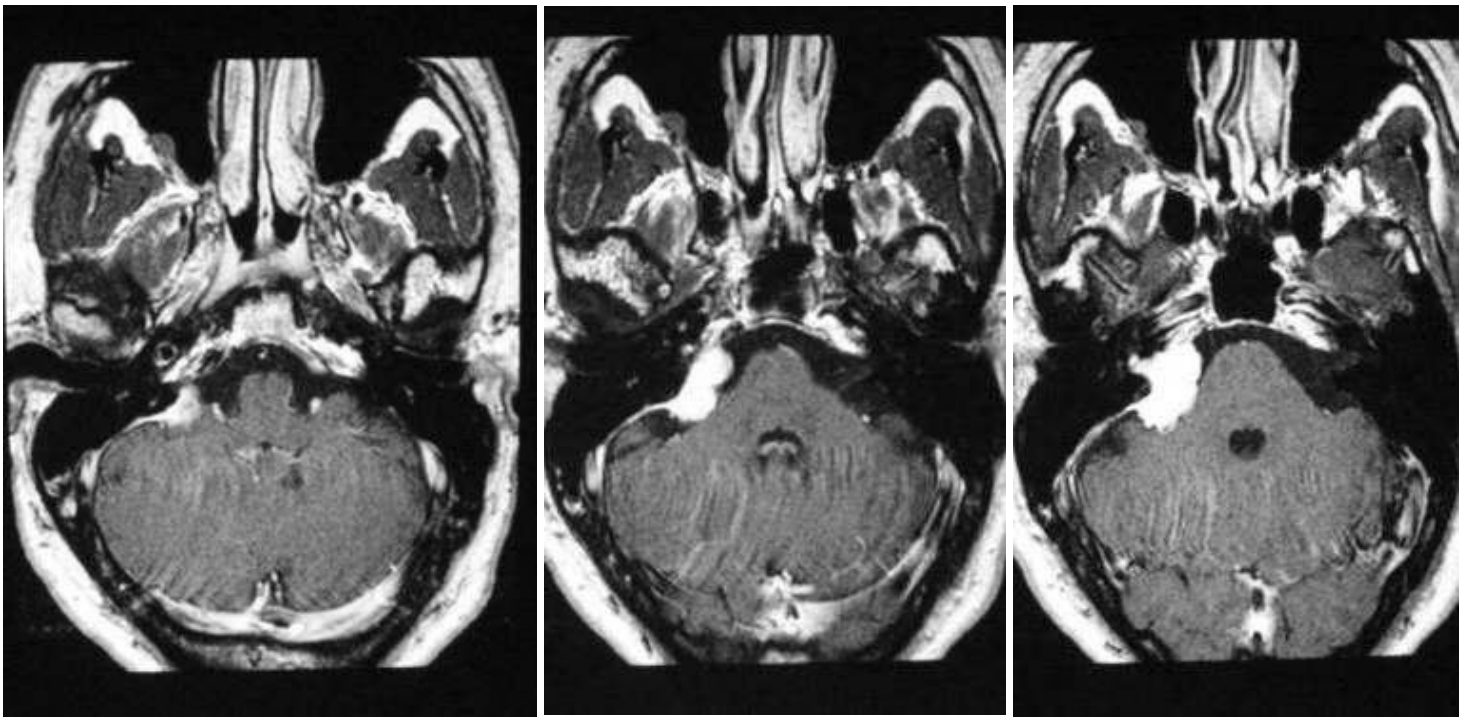

Figure 1. Postcontrast MRI T1 images showing a densely enhanced cerebellopontine angle meningioma, Notice the wide base attachment, the enhanced meningeal tail, and the moderate compression of the brain stem. A CSF cleft is also evident.

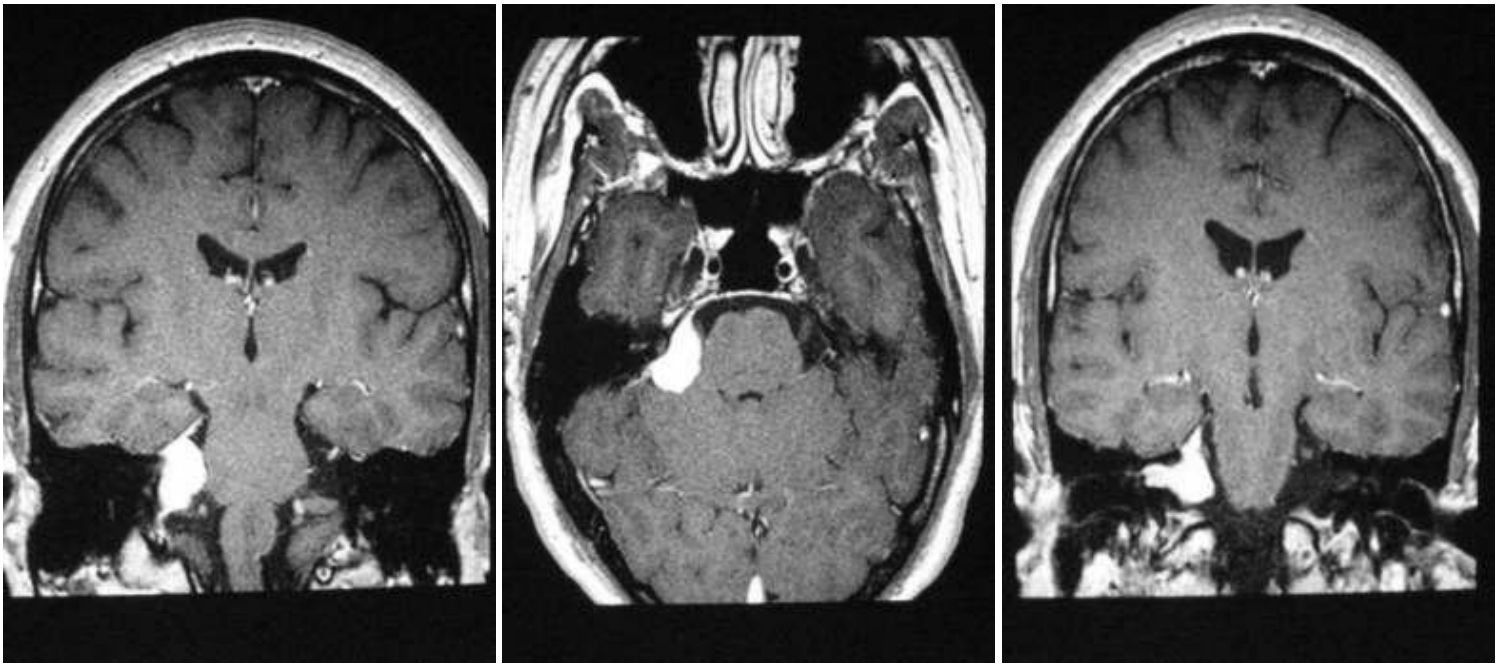

Figure 2. **Postcontrast MRI T1 images showing a densely enhanced cerebellopontine angle meningioma, Notice the wide base attachment, the enhanced meningeal tail, and the moderate compression of the brain stem. A CSF cleft is also evident.**

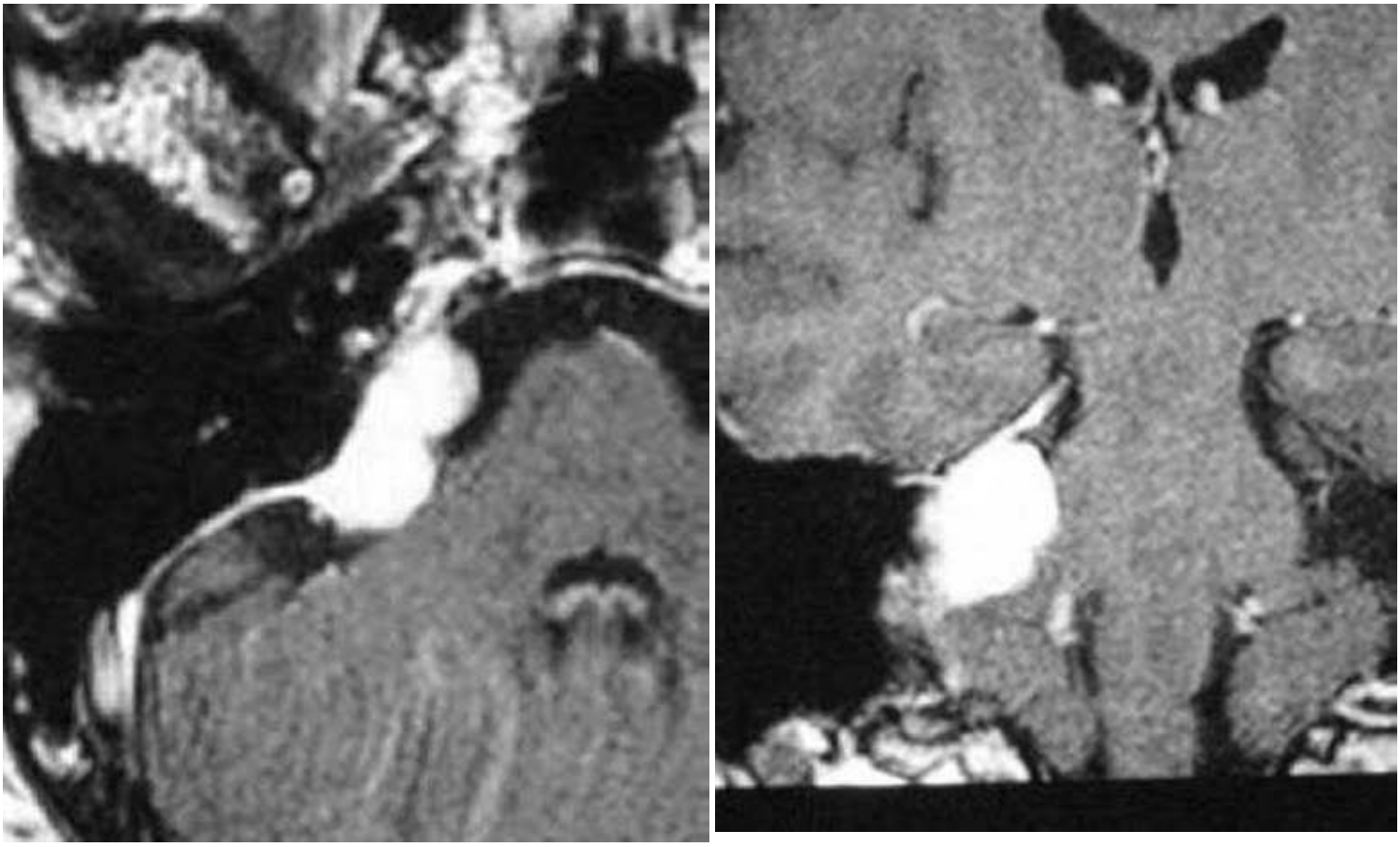

Figure 3. **Postcontrast MRI T1 images showing a densely enhanced cerebellopontine angle meningioma, Notice the wide base attachment, the enhanced meningeal tail, and the moderate compression of the brain stem. A CSF cleft is also evident.**

Figure 4. The meningioma (syncytial subtype) is hyperintense on the MRI T2 images

Table 1. MRI appearance of the various types of meningiomas

Type	Comment
Fibroblastic meningiomas	Fibroblastic meningiomas are composed of large, narrow spindle cells. The distinct feature is the presence of abundant reticulum and collagen fibers between individual cells. On MR imaging, fibroblastic meningiomas with cells embedded in a dense collagenous matrix appear as low signal intensity in Tl-weighted and T2-weighted pulse sequences.
Transitional meningiomas	Transitional meningiomas are characterized by whorl formations in which the cells are wrapped together resembling onion skins. The whorls may degenerate and calcify, becoming psammoma bodies. Marked calcifications can be seen in this histologic type. MR imaging of transitional meningiomas thus also demonstrates low signal intensity on Tl- weighted and T2-weighted images, with the calcifications contributing to the low signal intensity.
Syncytial meningiomas	Syncytial (meningothelial, endotheliomatous) meningiomas contain polygonal cells, poorly defined and arranged in lobules. Syncytial meningiomas composed of sheets of contiguous cells with sparse interstitium might account for higher signal intensity in T2-weighted images. Microcystic changes and nuclear vesicles can also contribute to increased signal intensity.
Angioblastic meningiomas	Angioblastic meningiomas are highly cellular and vascular tumors with a spongy appearance. Increased signal in T2-weighted pulse sequence of these tumors is due to high cellularity with increase in water content of tumor.

Thus based on the correlation between histology and MR imaging appearance of meningiomas, it has been concluded that meningiomas significantly hyperintense to cortex tend to be primarily of syncytial or angioblastic type, whereas meningiomas hypointense to cortex tend to be primarily of fibrous or transitional type. Heterogeneous appearance of meningiomas in T2-weighted pulse sequence can be due to tumor vascularity, calcifications, and cystic foci.

Table 2. MRI characteristics of meningiomas

Pathological type	T2 MRI appearance

Fibroblastic	**Hypointense on the T2 images because of the existence of dense collagen and fibrous tissue**
Transitional	**Hypointense on the T2 images because of the existence of densely calcified psammoma bodies**
Syncytial	**Hyperintense on the T2 images because of the existence of high cell count, microcysts or significant tissue oedema**
Angioblastic	**Same as the syncytial type. Blood vessels appear as signal void convoluted structures**

Table 3. MRI characteristics of meningiomas

MRI feature	Description
Vascular rim	**The peripheries of meningiomas are supplied by branches from the anterior or middle cerebral arteries that encircle the tumour and form the characteristic vascular rim**
Meningeal tail	**The tail extends to a variable degree away from the meningioma site and probably represents a meningeal reaction to the tumour**
Hypointense cleft	**Hypointense cleft between the tumour and the brain that probably represents blood vessels or a CSF interface**

- **The dural tail or "dural flair"**

The dural tail is a curvilinear region of dural enhancement adjacent to the bulky hemispheric tumor. The finding was originally thought to represent dural infiltration by tumor, and resection of all enhancing dura mater was thought to be appropriate. However, later studies helped confirm that most of the linear dural enhancement, especially when it was more than a centimeter away from the tumor bulk, was probably caused by a reactive process. This reactive process includes both vasocongestion and accumulation of interstitial edema, both of which increase the thickness of the dura mater. Because the dural capillaries are "nonneural," they do not form a blood-brain barrier, and, with accumulation of water within the dura mater, contrast material enhancement occurs.

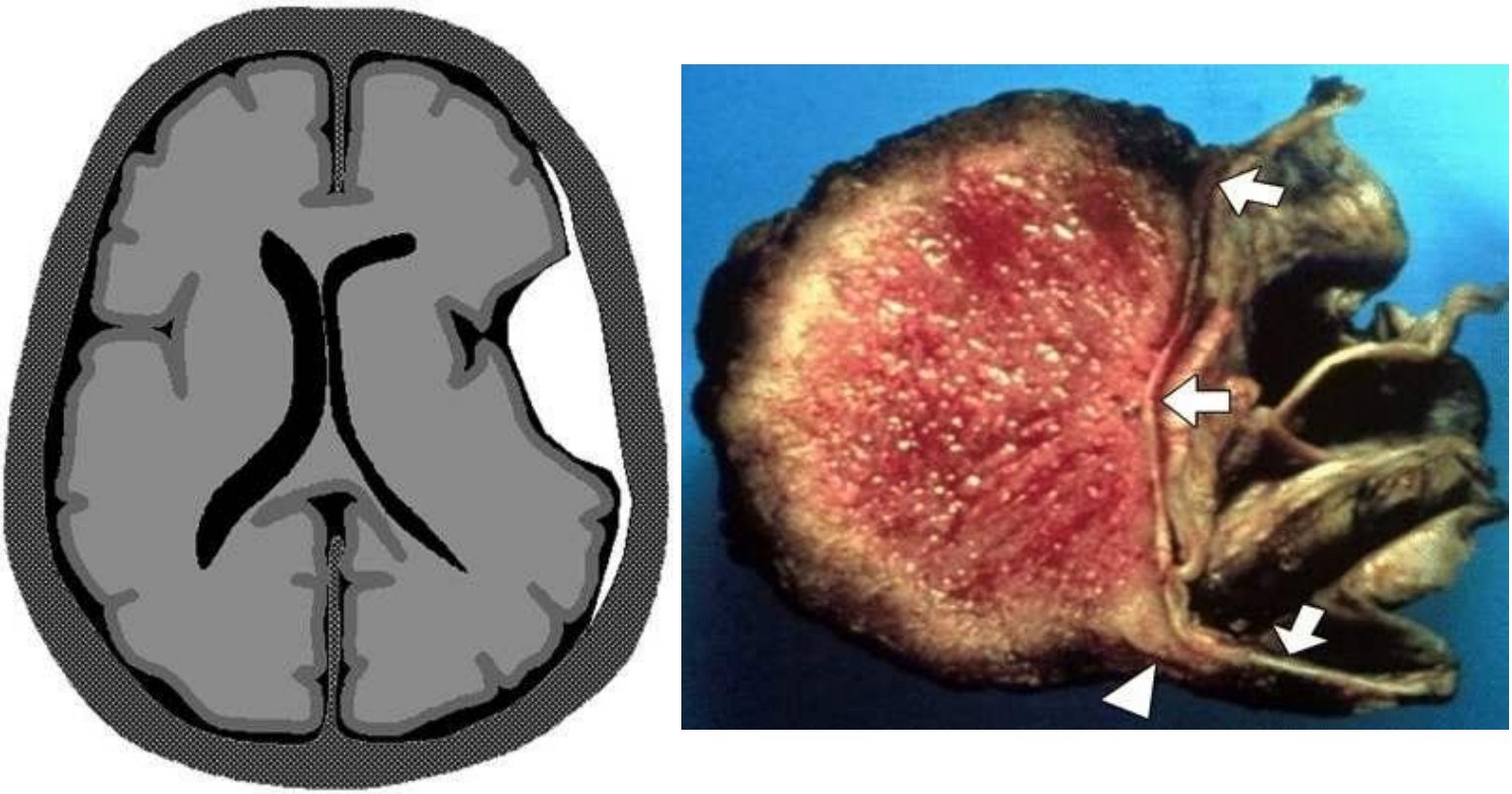

Figure 5. Dural tail enhancement with meningioma. (a) Diagram illustrates the thin, relatively curvilinear enhancement

that extends from the edge of a meningioma. Most of this enhancement is caused by vasocongestion and edema, rather than neoplastic infiltration. The bulk of the neoplastic tissue is in the hemispheric extraaxial mass; nonetheless, the dural tail must be carefully evaluated at surgery to avoid leaving neoplastic tissue behind. (b) Photograph of a resected meningioma shows the dense, "meaty," well-vascularized neoplastic tissue. At the margin of the lesion, there is a "claw" of neoplastic tissue (arrowhead) overlying the dura mater (arrows) that is not directly involved with tumor.

DIAGNOSIS:

DIAGNOSIS: CEREBELLOPONTINE ANGLE MENINGIOMA

DISCUSSION

DISCUSSION:

Lesions that arise within or involve the internal auditory canal (IAC) can be considered together with lesions affecting the cerebellopontine angle (CPA) cistern. This group of lesions consists of neoplastic and cystic masses arising from normal or ectopic structures in the CPA region and also inflammatory and vascular processes that affect the CPA and IAC cisterns and the cranial nerves located there. In addition to lesions specific to this region, any intraaxial or extraaxial process that involves subarachnoid cisternal spaces in general can also be seen here.

- **Vestibulocochlear schwannoma**

Vestibulocochlear schwannoma (VCS) is a benign, slowly growing neoplasm that arises from Schwann cells in the nerve sheath of the vestibulocochlear nerve. This tumor can affect other cranial nerves, but has a predilection for the eighth nerve, and in particular the vestibular portion of the nerve, which has led to the preferred use of the term VCS rather than the well-known synonym, acoustic neuroma [2]. The majority of intracranial schwannomas affect the vestibular portion of the eighth nerve, and only a minority affect the cochlear portion.

VCS is a common tumor, accounting for approximately three fourths of all CPA masses and approximately one tenth of all intracranial tumors [3,4]. Patients with VCS usually present in the fourth to sixth decades. The most common symptom is progressive unilateral SNHL, often accompanied by tinnitus [5]. Vestibular symptoms of vertigo and dizziness are less common, which is curious given that most of these tumors arise from the vestibular portion of the nerve. This phenomenon may be because of a lesser susceptibility of the nerve to the effects of compression or because of the central nervous system's better ability to compensate for unilateral vestibular denervation [6]. Very large tumors in the CPA also may present with symptoms of cerebellar dysfunction or neuropathy of the lower cranial nerves.

VCS is associated with neurofibromatosis type 2 (NF-2) [7], and this condition should be suspected when VCS is bilateral or is discovered in a child or young adult. The presence of NF-2 should also heighten the radiologist's awareness of possible associated lesions, including meningiomas and ependymomas. Malignant degeneration of VCS is rare and is associated with NF-1 [8]. Melanotic schwannoma is another malignant variant of VCS that may arise from melanocytes that share their neural crest origin with Schwann cells [9].

MRI is the preferred imaging modality for detecting and describing VCS, unless MRI is contraindicated. [10]. On unenhanced T1WI, schwannomas appear isointense to brain and can usually be detected as masses that displace the normal CSF signal. After contrast administration, schwannomas typically show uniform enhancement, although heterogeneity may be seen when areas of internal cystic or hemorrhagic change are present [11].

VCSs typically are centered near the porus acusticus and classically are described as having an elongated intracanalicular component and bulbous CPA cisternal component that result in an “ice cream cone” configuration (Fig. 1). Small lesions that are 15 mm or less may be contained entirely within the IAC and have a tubular shape [12]. Large lesions that are 30 mm or greater typically have a dominant CPA component. VCSs usually are solid but may show cystic or hemorrhagic change, particularly in large or rapidly growing tumors [13] (Fig. 2).

Figure 6. Vestibulocochlear schwannoma. Axial T1-weighted MR imaging with contrast in patient with progressive SNHL shows an intensely enhancing schwannoma that nearly fills the IAC. The bulbous rounded portion of the tumor proximally projects into the CPA.

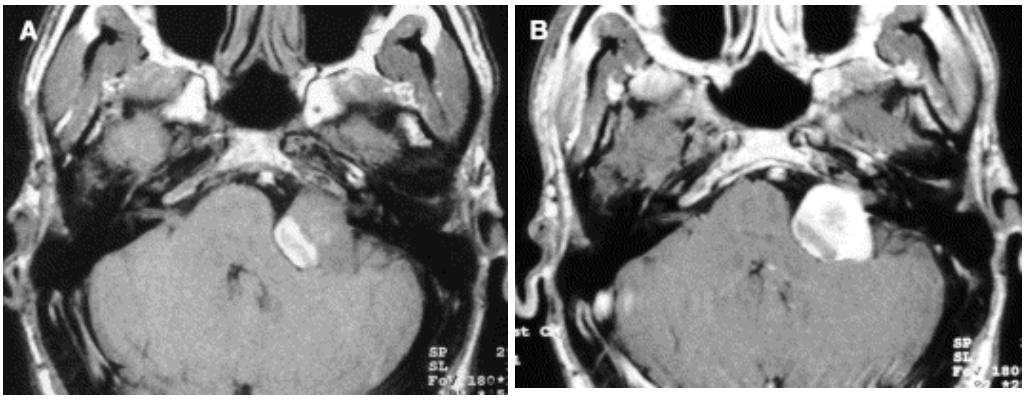

Figure 7. Vestibulocochlear schwannoma. (A) Axial T1-weighted MR imaging without contrast. Intrinsic high T1 signal in the posteromedial portion of the CPA tumor represents subacute blood products as a result of hemorrhage in this schwannoma. (B) Postcontrast image demonstrates typical intense enhancement in the remainder of the tumor.

Contrast-enhanced MRI is considered widely to be the first-line imaging technique for VCS evaluation, because of the sensitivity afforded by the intense enhancement that these tumors typically manifest, even in small lesions [14]. High-resolution T2 FSE imaging is, however, a supplemental noncontrast technique that can provide exquisite imaging of the CSF and nerves in the CPA and IAC. On T2 FSE, VCSs appear as nodules or filling defects against the background of bright CSF (Fig. 3). This technique allows for detection of tumors as small a few millimeters and can provide adjunctive information that is useful in surgical planning, such as identifying from which nerve component the tumor arises, defining the exact extent of the tumor boundaries, and whether there is a CSF cap at the fundus of the IAC. In the proper clinical setting, T2 FSE can serve as an inexpensive screening technique for patients with uncomplicated SNHL [15].

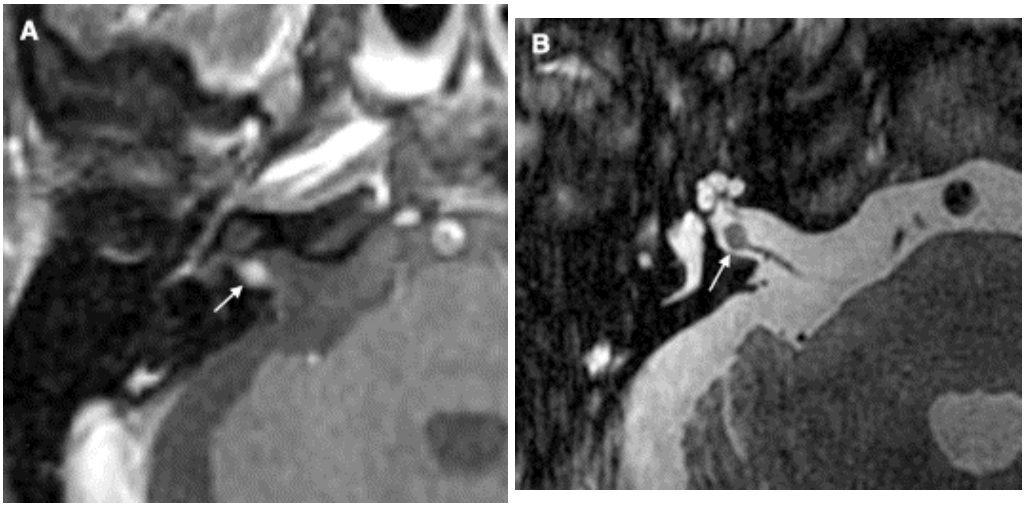

Figure 8. Vestibular schwannoma. (A) Axial T1-weighted postcontrast image of the IAC. Enhanced image demonstrates a nodule of intense enhancement, corresponding to a small intracanalicular schwannoma. (B) Axial high-resolution T2 FSE MR image clearly demonstrates the tumor nodule, which originates from the inferior vestibular branch of the eighth cranial nerve.

- **Meningioma**

Meningiomas are neoplasms that arise from arachnoid cap cells, dural fibroblasts, or arachnoid membrane [16]. The latter accounts for lesions in the CPA region. These tumors typically are benign and well circumscribed and are epidemiologically and histologically similar to meningiomas that occur elsewhere in the cranial vault.

The incidence of meningioma in the CPA region is a distant second to VCS, accounting for approximately 5% to 10%

of CPA masses [17,18]. Depending on their location, CPA meningiomas may present with cranial neuropathy, cerebellar dysfunction, or other symptoms resulting from local mass effect. Rarely, a meningioma that is limited to the IAC may mimic clinically a VCS [19].

On noncontrast CT, meningiomas may be isointense or hyperintense, and unlike schwannomas, may show calcification in up to one fourth of lesions [20]. The presence of hyperostosis on CT also suggests a diagnosis of meningioma. On MRI, meningiomas show T1 signal that is roughly similar to brain and may be hyperintense or hypointense on T2WI. The hallmark imaging features of meningioma include extra-axial dural-based location, intense enhancement, hyperostosis, and calcification (Fig. 8). The dural origin of these tumors typically results in a hemispheric mass with a broad dural margin that forms an obtuse angle against the adjacent bone compared with the spheroid or nodular mass with acute angle typically seen in VCS [21,22]. The presence of a "dural tail" also favors the diagnosis of meningioma, although this sign is not totally specific [23]. A CPA meningioma also may extend into the IAC and differentiation between meningioma and VCS may be difficult (Fig. 9).

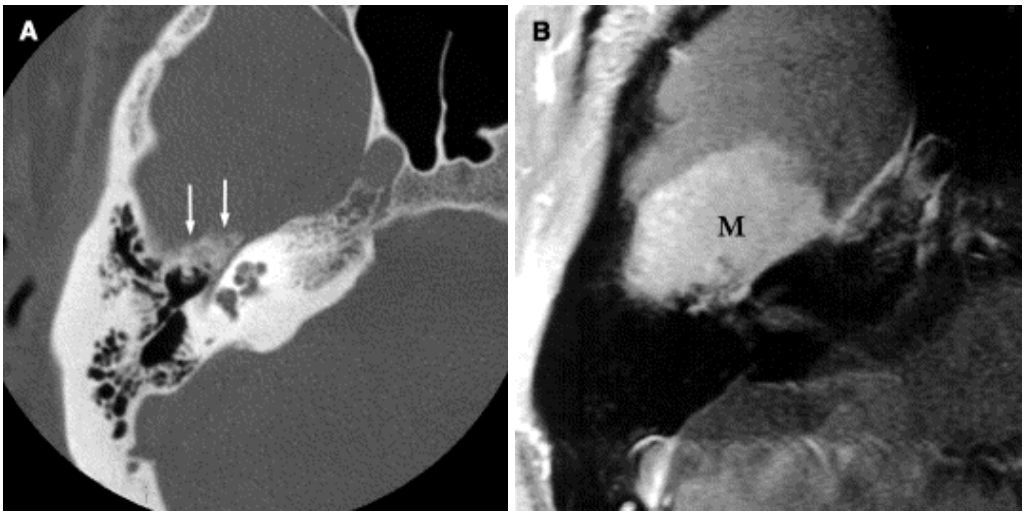

Figure 9. Meningioma. (A) Axial CT at bone algorithm of a patient with a temporal bone meningioma (M) centered over the petrous bone at the posterior floor of the middle cranial fossa. The hyperostotic bony changes (arrows) are characteristic for meningioma. (B) Postcontrast T1-weighted MR image shows characteristic enhancement.

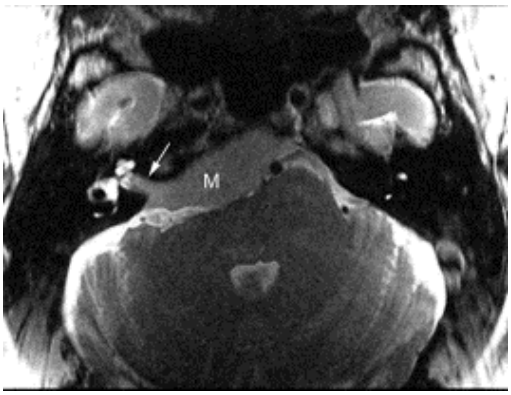

Figure 10. CPA meningioma. Axial high-resolution T2 FSE scan shows a broad dural-based extra-axial mass in the prepontine and CPA cisterns (M), with extension into the IAC (arrow).

- **Epidermoid and other cystic and congenital masses**
  - **Epidermoid cyst**

Epidermoid cyst (EC), also known as congenital cholesteatoma or epidermoid tumor, is caused by congenital rests of ectoderm in the CPA cistern. EC also can occur in the ventricles, petrous bone, tympanic cavity, skull base, and calvarium [24]. The squamous epithelium in these rests of ectoderm gives rise to accumulations of desquamated keratin debris. This keratinaceous material grossly has a glistening, pearly appearance that has led to this lesion called "the beautiful tumor" [25]. Patients with epidermoid typically present with symptoms in young or middle adulthood.

EC shows CT density that is similar to or slightly greater than that of CSF. On MR imaging, EC appears fairly homogeneous, with signal characteristics that are similar to CSF. On T1WI, EC is hypointense but usually slightly brighter than CSF, giving rise to the term "dirty CSF." In contrast to other CPA region tumors, EC does not enhance. EC is characteristically very hyperintense on T2WI and in some cases may be indistinguishable from CSF. When conventional MR imaging sequences are indeterminate, diffusion-weighted imaging can be useful and greatly increases the conspicuity of the lesion (Fig. 6).

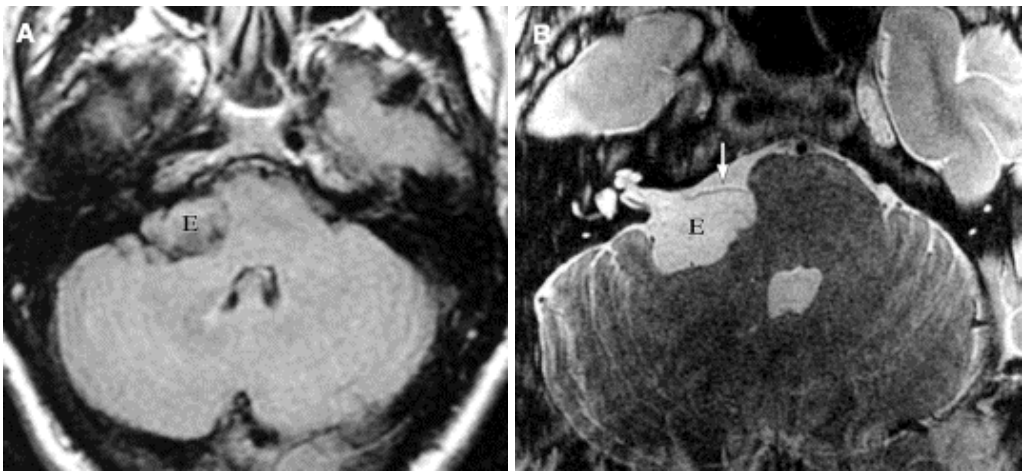

Figure 11. Epidermoid. (A) Axial T1-weighted image of the CPA region in a 35-year-old male with worsening vertigo. An epidermoid cyst is present (E), displacing the adjacent pons and cerebellum. The mass appears hyperintense relative to CSF. (B) Axial high-resolution T2 FSE MR imaging allows identification of the vestibulocochlear nerves and demonstrates anterior displacement of the cochlear branch (arrow) by the epidermoid cyst. The mass shows T2 signal identical to CSF.

- **Arachnoid cysts (AC)**

Arachnoid cysts (AC) are simple loculated CSF collections that form as a result of a congenital focal defect or duplication of the arachnoid membrane [26]. ACs can be seen in any location where the arachnoid membrane is found, but the some of the more common locations include the middle cranial fossa, sylvian cisterns, and hemispheric convexities. Less common locations include the CPA cisterns, suprasellar cistern, and cisterna magna. The imaging features of AC are those of a large uniform CSF collection with smooth rounded margins. AC appears isodense to CSF on CT and isointense to CSF on T1WI and T2WI, showing no contrast enhancement. AC may appear similar to EC. Mass affect on adjacent brain or mild remodeling of adjacent bone often are present (Fig. 7). When the cyst wall cannot be seen, differentiation between a simple enlarged CSF space and a small AC can be difficult.

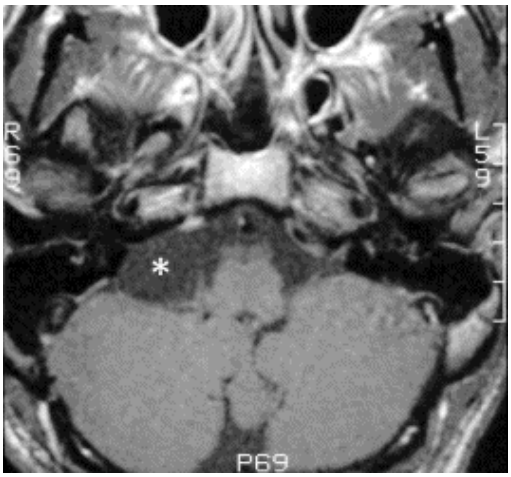

Figure 12. Arachnoid cyst. Axial T1-weighted MR images through the CPA cistern demonstrate a homogeneous CSF-signal collection () that causes mild mass effect on the adjacent brain structures. The cyst wall is incompletely perceptible.

- **Dermoid cyst (DC)**

Dermoid cyst (DC) is similar to EC in that it is the result of a congenital ectodermal inclusion, but differs in that it includes tissues from all three ectodermal layers. DCs may contain fat, dermal appendages (including hair and teeth), and calcification. DCs may rupture, resulting in spread of contents in the subarachnoid space and causing a chemical meningitis.

- **Lipomas**

Lipomas are congenital hamartomatous lesions that are distinct from DCs. Lipomas are masses of ectopic fat that probably form as a result of fatty maldevelopment of primitive meningeal mesodermal tissues [27]. Intracranial lipomas most commonly are seen at the midline, often in association with callosal or other midline anomalies, but can also occur in the CPA region [28]. Lipomas located within the IAC have been described [29]. Both DCs and lipomas on MRI show characteristic hyperintense fat signal on T1WI. Lipomas tend to be smaller and more homogeneous (Fig. 8). DCs often contain heterogeneous elements, including calcification, which is best appreciated CT. DC typically has greater mass effect and may rupture, producing a characteristic appearance of scattered fat droplets in the CSF space.

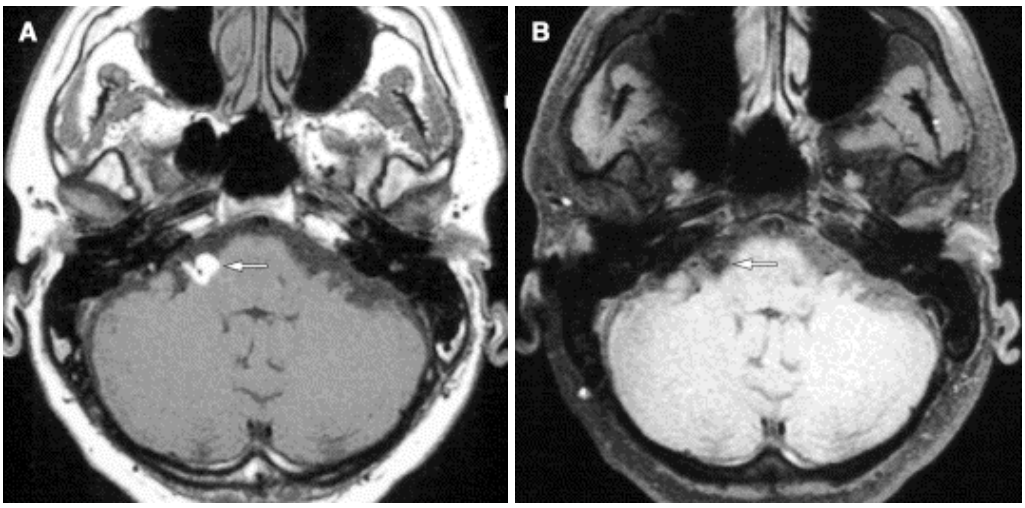

Figure 13. Lipoma. (A) Axial T1-weighted MR image shows a CPA mass (arrow) with intrinsic T1 hyperintensity that is characteristic of lipoma. (B) Axial T1-weighted MR imaging with fat suppression confirms the fatty nature of the mass.

- **Malignant and inflammatory meningitides**

Any process that affects the meninges and subarachnoid spaces generally can affect the CPA and IAC cisterns. Spread of malignancy to the subarachnoid space and CSF results in carcinomatosis and may be seen in patients with primary CNS malignancy, adenocarcinoma (especially breast and lung), lymphoma, melanoma, leukemia, or other metastatic malignancy [30]. Infectious meningitis, particularly tuberculous and fungal meningitis, results in focal meningeal disease that is most prominent in the basilar cisterns. Noninfectious inflammatory conditions also cause localized meningeal changes, including sarcoidosis, histiocytosis, idiopathic hypertrophic pachymeningitis, and postoperative meningeal reaction [31–34].

Meningeal disease is evaluated best with contrast-enhanced MR imaging. Abnormal enhancement may appear as multiple nodular deposits or as focal or diffuse leptomeningeal or pachymeningeal thickening [35,36] (Fig. 9). A solitary meningeal deposit may mimic meningioma [37]. In general, when a focal meningeal process is discovered in the CPA or IAC, the remainder of the intracranial contents and spinal axis should be examined to evaluate for possible involvement.

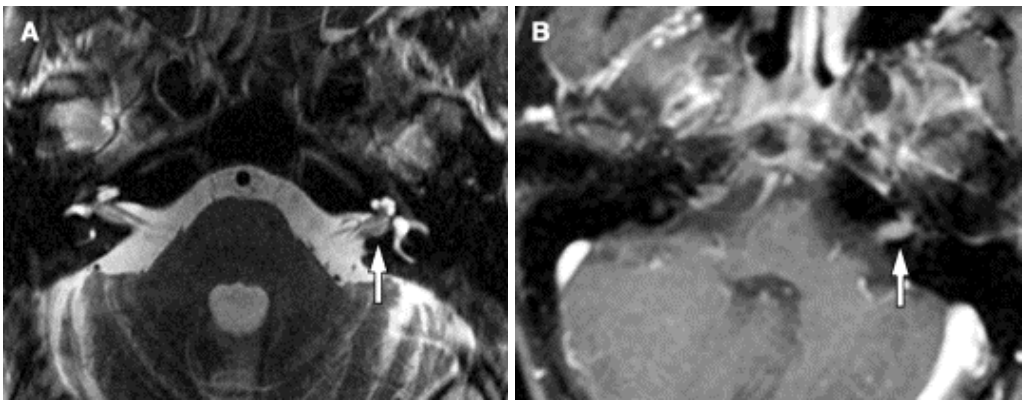

Figure 14. IAC metastasis. (A) Axial T2 FSE image of the temporal bone in an elderly woman with acute onset hearing loss. Ill-defined thickening of the nerves in the IAC is seen. (B) Axial-enhanced T1-weighted image shows enhancement in the IAC as a result of carcinomatous implant. Bilateral IAC and additional cisternal enhancement were also present (not shown).

- **Glomus tympanicum paraganglioma**

Glomus tympanicum paraganglioma (GTP) is tumor of glomus cells, or paraganglia, that reside in the inferior temporal bone. GTP is a subtype of paraganglioma that is localized to the glomus formations of the glossopharyngeal (Jacobson's nerve) that are found near the cochlear promontory. Paragangliomas, which are located in the jugular foramen, the proximal carotid sheath, and carotid bifurcation, are referred to as glomus jugulare, glomus vagale, and carotid body tumor, respectively; the unique features of these lesions are not included in this discussion. When a large glomus jugulare extends into the middle ear, the term "glomus jugulotympanicum" is used.

GTP is three times more common in women than men, usually presenting in middle age. Patients typically present with pulsatile tinnitus, conductive hearing loss, or inner ear symptoms. Large jugulotympanicum tumors also may present with multiple lower cranial neuropathies. On otologic examination, GTP appears as a vascular retrotympanic mass.

Small GTP tumors are seen readily on thin-section CT. The lesion appears a nodule of soft tissue at the medial wall of

the middle ear, classically located at the cochlear promontory (Fig. 10). Larger tumors fill the middle ear, but typically do not cause bone erosion and tend to spare the ossicles. Glomus tumors show intense enhancement on MR imaging because of their vascular nature. MR imaging plays a critical role in defining the extension of GTP intracranially and into the skull base, inasmuch as the surgeon can appreciate only the tympanic part of the tumor on otoscopy.

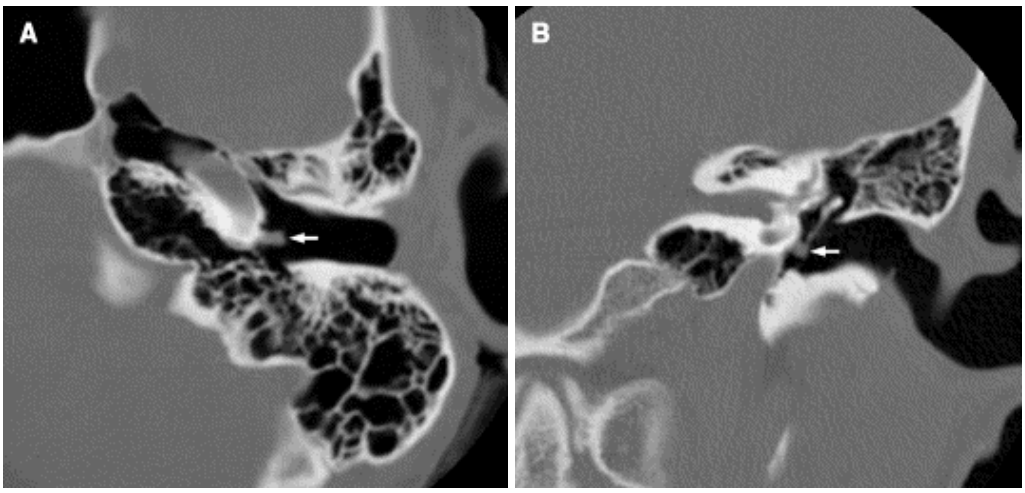

Figure 15. Glomus tympanicum paraganglioma. (A, B) Axial and coronal CT in a 36-year-old woman with pulsatile tinnitus and retrotympanic mass on otoscopic examination. A small soft-tissue mass is present at the medial wall of the middle ear overlying the lower portion of the cochlear promontory (arrows).

SUMMARY

SUMMARY

Meningiomas constitute between 13% and 19% of intracranial tumors. They are the most common tumors of nonglial origin. These tumors most often occur in patients between the ages of 40 and 70 years. They are twice as common in females. Meningiomas usually arise from the arachnoid, and there is a predilection for occurrence near arachnoid granulations. Deep within the adult brain, the most frequent sites of occurrence are from the tuberculum sellae, suprasellar and parasellar regions, sphenoid ridge, and tentorial incisura and the cerebellopontine angle. Intraventricular tumors are also described. These arise from the tela choroidea or from meningeal cell rests in the choroid plexus. They usually arise within the lateral ventricles and are more common on the left.

One of the keys to diagnosis of meningiomas is to recognize their extraaxial location. On CT, meningiomas usually appear as homogeneous hyperdense masses. Approximately 20% of meningiomas show some calcification, which is psammomatous in nature. About 10% of meningiomas are heterogeneous in density, which may reflect numerous intratumoral blood vessels or intratumoral cysts or cysts adjacent to the tumor. These usually occur in the angioblastic type. The vast majority of tumors show contrast enhancement, and peritumoral edema is common.

On MR imaging, meningiomas are isointense to gray matter in the majority of cases or mildly hypointense to gray matter on Tl-weighted images. Heavily T2- weighted images show that these tumors are either isointense (50%) or mildly hyperintense (40%) to gray matter. MR imaging is particularly helpful in delineating the extra-axial location of these tumors. It may show a cerebrospinal fluid cleft between the tumor and adjacent brain or directly visualize the displaced dural margins or pial vessels. A broad-based dural margin is frequently visible,the tentorial incisura is frequently thickened.

- **Addendum**
  - A new version of this PDF file (with a new case) is uploaded in my web site every week (every Saturday and

remains available till Friday.)

- To download the current version follow the link "http://pdf.yassermetwally.com/case.pdf".
- You can also download the current version from my web site at "http://yassermetwally.com".
- To download the software version of the publication (crow.exe) follow the link: http://neurology.yassermetwally.com/crow.zip
- The case is also presented as a short case in PDF format, to download the short case follow the link: http://pdf.yassermetwally.com/short.pdf
- At the end of each year, all the publications are compiled on a single CD-ROM, please contact the author to know more details.
- Screen resolution is better set at 1024*768 pixel screen area for optimum display.
- For an archive of the previously reported cases go to www.yassermetwally.net, then under pages in the right panel, scroll down and click on the text entry "downloadable case records in PDF format"
- Also to view a list of the previously published case records follow the following link (http://wordpress.com/tag/case-record/) or click on it if it appears as a link in your PDF reader

---

REFERENCES

References

[1]. Curtin HD, Som PM, Bergeron RT. Temporal bone embryology and anatomy. In: Som PM, Curtin HD, eds. (3rd edition) Head and neck imaging. volume 2:: Mosby-Year Book 1996:1330-1338

[2]. National Institutes of Health Consensus Development Conference Statement on Acoustic Neuroma. December 11–13, 1991. The Consensus Development Panel. Arch Neurol. 1994;51:201-207

[3]. Lo WWM, Solti-Bohman LG. Tumors of the temporal bone and the cerebellopontine angle. In: Som PM, Curtin HD, eds. (3rd edition) Head and neck imaging. volume 2:St. Louis: Mosby-Year Book 1996:1450

[4]. Swartz JD, Harnsberger HR. Imaging of the temporal bone. New York: Thieme Medical 1998p. 420

[5]. Kasantikul V, Netsky MG, Glassock Jr. ME, Hayes JW. Acoustic neurilemmoma. Clinicoanatomical study of 103 patients. J Neurosurg. 1980;52:28-35

[6]. Weissman JL. Hearing loss. Radiology. 1996;199:593-611

[7]. Lo WWM, Solti-Bohman LG. Tumors of the temporal bone and the cerebellopontine angle. In: Som PM, Curtin HD, eds. (3rd edition) Head and neck imaging. volume 2:St.Louis: Mosby-Year Book 1996:1451

[8]. Gruskin P, Carberry JN. Pathology of acoustic tumors. In: House WF, Luetze CM, eds. Acoustic tumors. volume 1:Baltimore: University Park Press 1979:85-148

[9]. Earls JP, Robles HA, McAdams HP, Rao KC. General case of the day. Malignant melanotic schwannoma of the eighth cranial nerve. Radiographics. 1994;14:1425-1427

[10]. Curtin HD. CT of acoustic neuroma and other tumors of the ear. Radiol Clin North Am. 1984;22:77-105

[11]. Tali ET, Yuh WT, Nguyen HD, et al. Cystic acoustic schwamnomas: MR characteristics. AJNR Am J Neuroradiol. 1993;14:1241-1247

[12]. Harnsberger HR. The lower cranial nerves. Handbook of head and neck imaging. (2nd edition) Chicago: Mosby-Year Book 1995:488-521

[13]. Charabi S, Mantoni M, Tos M, Thomson J. Cystic vestibular schwannomas: neuroimaging and growth rate. J Laryngol Otol. 1994;108:375-379

[14]. Curati WL, Graif M, Kingsley DP, et al. Acoustic neuromas: Gd-DTPA enhancement in MR imaging. Radiology. 1986;158:447-451

[15]. Allen RW, Harnsberger HR, Shelton C, et al. Low-cost high-resolution fast spin-echo MR of acoustic schwannoma: An alternative to enhanced conventional spin-echo MR?. AJNR Am J Neuroradiol. 1996;17:1205-1210

[16]. Black PM. Meningiomas. Neurosurgery. 1993;32:643-657

[17]. Hasso AN, Smith DS. The cerebellopontine angle. Semin Ultrasound CT MR. 1989;10:280-301

[18]. Lo WWM. Cerebellopontine angle tumors. San Diego (CA): Categorical Course on Neoplasms of the Central Nervous System. American Society of Neuroradiology; 1990.

[19]. Langman AW, Jackler RK, Althaus SR. Meningioma of the internal auditory canal. Am J Otol. 1990;11:201-204

[20]. Valavanis A, Schubiger O, Hayek J, Pouliadis G. CT of meningiomas on the posterior surface of the petrous bone. Neuroradiology. 1981;22:111-121

[21]. Lalwani AK, Jackler RK. Preoperative differentiation between meningioma of the cerebellopontine angel and acoustic neruoma suing MR imaging. Otolaryngol Head Neck Surg. 1993;109:88-95

[22]. Mikhael MA, Ciric IS, Wolff AP. Differentiation of cerebellowpontine angle neuromas and meningiomas with MR imaging. J Comput Assist Tomogr. 1985;9:852-856

[23]. Goldsher D, Litt AW, Pinto RS, et al. Dural "tail" associated with meningiomas on Gd-DTPA enhanced MR images: characteristics, differential diagnostic value, and possible implicatins for treatment. Radiology. 1990;176:447-450

[24]. Zimmerman RA, Bilaniuk LT, Dolinskas C. Cranial computed tomography of epidermoid and congenital fatty; tumors of maldevelopmental origin. J Comput Tomogr. 1979;3:40-50

[25]. Osbom AG. Diagnostic neuroradiology. St. Louis: Mosby 1994p. 631

[26]. Rock IP, Zimmerman R, Bell WO, Fraser RA. Arachnoid cysts of the posterior fossa. Neurosurgery. 1986;18:176-179

[27]. Smimiotopoulos JG, Yue NC, Rushing El. Cerebellopontine angle masses: radiologic-pathologic correlation. Radiographics. 1993;13:1131-1147

[28]. Dalley RW, Robertson WD, Lapointe JS, Durity FA. Computed tomography of a cerebellopontine angle lipom. J Comput Assist Tomogr. 1986;10:704-706

[29]. Cohen TI, Powers SK, Williams Jr. DW. MR appearance of intracanalicular eighth nerve lipoma. AJNR Am J Neuroradiol. 1992;13:1188-1190

[30]. Russell DS, Rubinstein LJ. Pathology of tumors of the nervous system. Baltimore: Williams & Wilkins 1989

[31]. Song SK, Schwartz IS, Strauchen JA, et al. Meningeal nodules with features of extranodal sinus histiocytosis with massive lymphadenoopathy. Am J Surg Pathol. 1989;13:406-412

[32]. Ranoux D, Devaux B, Lamy C, et al. Meningeal sarcoidosis, pseudo-meningioma, and pachymeningitis of the convexity. J Neurol Neurosurg Psychiatry. 1992;55:300-303

[33]. Mayer SA, Yim GK, Onesti ST, et al. Biopsy-proven isolated sarcoid meningitis. Case report. J Neurosurg. 1993;78:994-996

[34]. Martin N, Masson C, Henin D, et al. Hypertrophic cranial pachymeningitis: assessment with CT and MR imaging. AJNR Am J Neuroradiol. 1989;10:477-484

[35]. Sze G. Diseases of the intracranial meninges: MR imaging features. AJR Am J Roentgenol. 1993;160:727-733

[36]. Sze G, Soletsky S, Bronen R, Krol G. MR imaging of the cranial meninges with emphasis on contrast enhancement and meningeal carcinomatosis. AJNR Am J Neuroradiol. 1989;10:965-975

[37]. Buff Jr. BL, Schick RM, Norrgaard T. Meningeal metastasis of leiomyosarcoma mimicking meningioma: CT and MR findings. J Comput Assist Tomogr. 1991;15:166-167

[38]. Lefebvre PP, Leprince P, Weber T, et al. Neuronotrophic effect of developing otic vesicle on cochleo-vestibular neurons: evidence for nerve growth facto involvement. Brain Res. 1990;507:254-260

[39]. Casselman JW, Offeciers FW, Govaerts PJ, et al. Aplasia and hypoplasia of the vestibulocochlear nerve: diagnosis with MR imaging. Radiology. 1997;202:773-781

[40]. Glastonbury CM, Davidson HC, Harnsberger HR. Identification of deficiency of the cochlear nerve in patients with sensorineural hearing loss using t2 fast-spin echo imaging. Presented at the American Society of Neuroradiology, 37th Annual Meeting, May 1999, San Diego, CA.

[41]. Kim HS, Kim DI, Chung IH, Lee WS, Kim KY. Topographical relationship of the facial and vestibulocochlear nerves in the subarachnoid space and internal auditory canal. AJNR Am J Neuroradiol. 1998;19(6):1155-1161

[42]. Schuknecht HF. Pathology of the ear. (2nd edition) Philadelphia: Lea & Febiger 1993p. 332

[43]. Arnesen AR, Osen KK, Mugnaini E. Temporal and spatial sequence of anterograde degeneration in the cochlear nerve fibers of the cat. A light microscopic study. J Comp Neurol. 1978;178(4):679-696

[44]. Hoeffding V, Feldman ML. Degeneration in the cochlear nerve of the rat following cochlear lesions. Brain Res. 1988;449(1–2):104-115

[45]. Ylikoski J, Collan Y, Palva T. Pathologic features of the cochlear nerve in profound deafness. Arch Otolaryngol. 1978;104(4):202-207

[46]. Valvassori GE, Clemis JD. The large vestibular aqueduct syndrome. Laryngoscope. 1978;88:723-728

[47]. Jackler RK, De La Cruz A. The large vestibular aqueduct syndrome. Laryngoscope. 1989;99:1238-1243

[48]. Mafee MF, Charletta D, Kumar A, Belmont H. Large vestibular aqueduct and congenital SNHL. AJNR Am J Neuroradiol. 1992;13:805-819

[49]. Harnsberger HR, Dahlen RT, Shelton C. Advanced techniques in magnetic resonance imaging in the evaluation of the large vestibular aqueduct syndrome. Laryngoscope. 1995;105:1037-1042

[50]. Jackler RK, Luxford WM, House WF. Congenital malformations of the inner ear: a classification based on embryogenesis. Laryngoscope. 1987;97(pt 2, Suppl 40):2-14

[51]. Schuknecht HF. Pathology of the ear. Philadelphia: Lea & Febiger 1993p. 177

[52]. Schuknecht HF. Pathology of the ear. Philadelphia: Lea & Febiger 1993p. 115–189

[53]. Hasso AN, Casselman JW, Schmalbrock P. Temporal bone congenital anomalies. (3rd edition) In: Som PM, Curtin HD, eds. Head and neck imaging. volume 2:St. Louis: Mosby-Year Book 1996:1361-1367

[54]. Michel EM. Memoire sur les anomalies congenitales de l'oreille interne, avec la premiere observation authentique d'abscece complete d'oreille moyenne chez un sourd et muet de naissance, mort a l'age de onze ans. Gaz Med Strasb. 1863;23:55-58

[55]. Mondini C. Anatomia surdi nati sectio. De Bononiensi Scientiarum et Artium Instituto atzue Academia Commentarii. Bononiae. 1791;7:28-29419–31

[56]. Lemmerling MM, Mancuso AA, Antonelli PJ, Kubilis PS. Normal modiolus: CT appearance in patients with a large vestibular aqueduct. Radiology. 1997;204:213-219

[57]. Brogan M, Chakeres DW. Gd-DTPA-enhanced MR imaging of cochlear schwannoma. AJNR Am J Neuroradiol. 1990;11:407-408

[58]. Saeed SR, Birzgalis AR, Ramsden RT. Intralabyrinthine schwannoma shown by magnetic resonance imaging. Neuroradiology. 1994;36:63-64

[59]. Mark AS. Contrast-enhanced magnetic resonance imaging of the temporal bone. Neuroimaging Clin North Am. 1994;4:117-131

[60]. Davidson HC, Krejei CS, Hamsberger HR. MR evaluation of labyrinthine schwannomas. Presented at the American Society of Neuroradiology 36th Annual Meeting, Philadelphia, Apri1 1998.

[61]. Forton GE, Somers T, Hermans R, et al. Preoperatively diagnosed utricular neuroma treated by selective partial labyrinthiectomy. Ann Otol Rhinol Laryngol. 1994;103:885-888

[62]. Swartz JD. Temporal bone inflammatory disease. (3rd edition) In: Som PM, Curtin HD, eds. Head and neck imaging. Volume 2:St. Louis: Mosby-Year Book 1996:1415-1418

[63]. Seltzer S, Mark AS. Contrast enhancement of the labyrinth on MR scans in patients with sudden hearing loss and vertigo: evidence of labyrinthine disease. AJNR Am J Neuroradiol. 1991;12:13-16

[64]. Mark AS, Seltzer S, Nelson-Drake J, et al. Labyrinthine enhancement on gadolinium-enhanced magnetic resonance imaging in sudden deafness and vertigo: correlation with audiologic and electronystagmographic studies. Ann Otol Rhinol Laryngol. 1992;101:459-464

[65]. Mark AS. Contrast-enhanced magnetic resonance imaging of the temporal bone. Neuroimaging Clin North Am. 1994;4:117-131

[66]. Downie AC, Howlett DC, Koefman RJ, et al. Case report: prolonged contrast enhancement of the inner ear on magnetic resonance imaging in Ramsay Hunt syndrome. Br J Radiol. 1994;67:819-821

[67]. Davidson HC, Krejci CS, Harnsberger HR. MR Evaluation of labyrinthine schwannomas. Presented at the American Society of Neuroradiology 36th Annual Meeting, Philadelphia, April 1998.

[68]. Swartz JD, Hamsberger HR. Imaging of the temporal bone. New York: Thieme Medical Publishers 1998p. 272–82

[69]. Weissman JL, Kamerer DB. Labyrinthitis ossificans. Am J Otolaryngol. 1993;14:363-365

[70]. Paparella MM. Labyrinthitis. In: Paparella MM, Shumrick DA, eds. Otolaryngology: the ear. Volume 2:Philadelphia: WB Saunders 1980:1735-1756

[71]. Swartz JD, Mandell DW, Wolfson RJ, et al. Fenestral and cochlear otosclerosis. Computed tomographic evaluation. Am J Otolaryngol. 1985;6:476-481

[72]. Casselman JW, Kuhweide R, Ampe W, et al. Pathology of the membranous labyrinth: comparison of T1- and T2-weighted and gadolinium-enhanced spin-echo and 3DFT-CISS imaging. AJNR Am J Neuroradiol. 1993;14:59-69

[73]. Heffner DK. Low-grade adenocarcinoma of probable endolymphatic sac origin: a clinicopathologic study of 20 cases. Cancer. 1989;64:2292-2302

[74]. Batsakis JG, el-Naggar AK. Papillary neoplasms (Heffner's tumors) of the endolymphatic sac. Ann Otol Rhinol Laryngol. 1993;102(pt 1):648-651

[75]. MacDougal AD, Sangalang VE. A previously unrecognized papillary endolymphatic sac tumor presenting as a cerebellopontine angle lesion. Can J Neurol Sci. 1985;189:203-204

[76]. Palmer JM, Coker NJ, Harper RL. Papillary adenoma of the temporal bone in von Hippel-Lindau disease. Otolaryngol Head Neck Surg. 1989;100:64-68

[77]. Conley J, Janecka I. Schwan cell tumors of the facial nerve. Laryngoscope. 1974;84:958-962

[78]. Latack JT, Gabrielsen TO, Knake JE, et al. Facial nerve neruomas: radiologic evaluation. Radiology. 1983;149:731-739

[79]. Dort JC, Fisch U. Facial nerve schwanomma. Skull Base Surg. 1991;1:51-57

[80]. Pillsbury HC, Price HC, Gardiner LJ. Primary tumors of the facial nerve: diagnosis and management. Laryngoscope. 1983;93:1045-1048

[81]. Jackson CG, Glasscock 3rd ME, Sismanis A. Facial paralysis of neoplastic origin: diagnosis and management. Laryngoscope. 1980;90(pt 1):1581-1595

[82]. Nelson RA, House WF. Facial nerve neuroma in the posterior fossa: surgical considerations. In: Graham MD, House WF, eds. Proceedings of the Fourth International Symposium on Facial Nerve Surgery. New York: Raven 1982:403-406

[83]. Lidov M, Som PM, Stacy C, Catalano P. Eccentric cystic facial schwannoma: CT and MR features. J Comp Assist Tomogr. 1991;15:1065-1067

[84]. McMenomey SO, Glasscock 3rd ME, Nlinor LB, et al. Facial nerve neuromas presenting as acoustic tumors. Am J Otol. 1994;15:307-312

[85]. Davidson HC. Head and neck digital teaching file. Salt Lake City (UT): Electronic Medical Education Resource Group; 1999. Retrieved September 24, 2001, from DTF database.

[86] Metwally, MYM: Textbook of neuroimaging, A CD-ROM publication, (Metwally, MYM editor) WEB-CD agency for electronic publication, version 10.1a January 2009